

Polarized luminescence from Jahn-Teller split triplet states of self-trapped excitons in PbMoO₄

Minoru Itoh (伊藤 稔)* and Takushi Kajitani (梶谷拓史)

Department of Electrical and Electronic Engineering, Faculty of Engineering, Shinshu University, 4-17-1 Wakasato, Nagano 380-8553, Japan

(Received 6 December 2012; revised manuscript received 20 January 2013; published 8 February 2013)

The green luminescence from the triplet states of a self-trapped exciton (STE) located on a tetrahedral (MoO₄)²⁻ ion in PbMoO₄ splits into three bands, I, II, and III, as a result of the symmetry lowering of the (MoO₄)²⁻ ion due to a Jahn-Teller effect. Time-resolved luminescence measurements have been performed for polarizations with the electric vector parallel to the crystallographic *c* axis (**E**∥**c**) and perpendicular to it (**E**⊥**c**) in a temperature range between 8 and 225 K. All three bands are confirmed to exhibit significant polarizations. The main band II at 520 nm is polarized with **E**∥**c** at low temperatures (*T* < 75 K) but changes its polarization from **E**∥**c** to **E**⊥**c** at *T* > 125 K. Band III at 600 nm is polarized with **E**⊥**c** at *T* = 170 and 225 K. The degree of polarization of these two bands does not depend on the polarization of excitation light. On the other hand, band I at 405 nm is polarized with **E**⊥**c** (**E**∥**c**) under the excitation by photons polarized parallel (perpendicular) to the *c* axis, in the range of *T* = 150–225 K. The observation of polarized luminescence provides convincing evidence for further lowering of the symmetry of (MoO₄)²⁻ ions due to a uniaxial crystal field in addition to the Jahn-Teller distortion. The sublevels of the triplet STE state responsible for the PbMoO₄ luminescence are identified on the basis of group-theoretical considerations.

DOI: [10.1103/PhysRevB.87.085201](https://doi.org/10.1103/PhysRevB.87.085201)

PACS number(s): 78.55.Hx, 71.35.-y, 71.70.-d

I. INTRODUCTION

We have performed a series of studies on the nature of the excited state(s) of a self-trapped exciton (STE) in the family of transition-metal tungstates and molybdates by means of time-resolved luminescence spectroscopy. Both families crystallize in either a scheelite structure or wolframite structure.^{1,2} An STE created in the scheelite family is located on a tetrahedral (WO₄)²⁻ or (MoO₄)²⁻ molecular ion, while that in the wolframite family is located on a (WO₆)⁶⁻ or (MoO₆)⁶⁻ octahedra with shared oxygen ions.³ Since WO₄ (MoO₄) is isolated from each other and has a higher symmetry than WO₆ (MoO₆), we have focused our interest on the STEs in tungstates and molybdates with a scheelite structure.

Lead compounds PbWO₄ and PbMoO₄ are representatives of scheelite tungstates and molybdates, respectively. In these crystals, localization of the STE on a (WO₄)²⁻ or (MoO₄)²⁻ ion with tetrahedral symmetry *T_d* could result in four electronic states: two singlets with irreducible representations ¹*T*₁ and ¹*T*₂ and two triplets with irreducible representations ³*T*₁ and ³*T*₂.^{4,5} The energies of these excited states are thought to lie in the sequence ¹*T*₂ > ¹*T*₁ > ³*T*₂ ≅ ³*T*₁. The energy separation between ³*T*₂ and ³*T*₁ is expected to be very small, because in a first approximation the only difference is due to Coulomb integrals involving 2*p* oxygen orbitals.⁵ The ground singlet state transforms in *T_d* symmetry like ¹*A*₁. The energy-level diagram described above is schematically illustrated on the left side of Fig. 1. The intrinsic luminescence of PbWO₄ is peaked at 425 nm in the blue spectral region and that of PbMoO₄ appears at ~520 nm in the green spectral region. It has long been supposed^{6–10} that these intrinsic luminescence bands originate from the radiative transitions from the triplet ³*T*₁ and/or ³*T*₂ states to the ground ¹*A*₁ state. The ³*T*₁/³*T*₂ → ¹*A*₁ transition is spin forbidden but is partially allowed by the spin-orbit interaction with the upper-lying singlet ¹*T*_{1,2} states. This model, however, may not be satisfactory enough, because it does not take a Jahn-Teller (JT) effect into

consideration. The JT effect is a kind of spontaneous symmetry breaking in which an electronically degenerate complex upon excitation becomes unstable against distortions and removes its degeneracy inevitably.¹¹

Time-resolved spectroscopy on PbWO₄,^{12,13} PbMoO₄,¹⁴ and CdMoO₄¹⁵ has shown that the intrinsic luminescence in these materials is composed of three emission bands, I, II, and III, with different decay times. The appearance of three components reveals the importance of a JT effect on the triplet luminescence in scheelite tungstates and molybdates. The symmetry lowering of (WO₄)²⁻ or (MoO₄)²⁻ ions from *T_d* to *C_{3v}* due to the JT effect could lift the degeneracy of the ³*T*₂ and ³*T*₁ states, which results in four triplet sublevels, two of them being closely spaced in energy. These JT split sublevels are thought to correspond to three time-resolved components in PbWO₄, PbMoO₄, and CdMoO₄. This conclusion is fairly consistent with a theoretical study by Bacci *et al.*,^{16,17} who have suggested that owing to trigonal JT distortion, the lowest triplet state of PbWO₄ splits into three adiabatic potential energy surfaces in a configuration coordinate diagram. The importance of the JT effect on the excited triplet states of tetrahedral oxyanion molecules has also been pointed out through optically detected magnetic resonance experiments by van der Waals *et al.*^{18–20}

More detailed information on the electronic structure of the excited STE states has been drawn for PbWO₄ from the investigation of polarization properties of time-resolved luminescence spectra.²¹ Bands I, II, and III are all found to be characteristically polarized with respect to the crystallographic *c* axis. This finding is of great interest, because no polarization is expected for the STE luminescence as far as the (WO₄)²⁻ ion holds the *C_{3v}* symmetry. The result of PbWO₄, therefore, strongly suggests a crucial role of further symmetry lowering of the JT-distorted (WO₄)²⁻ ions. However, it does not provide enough evidence to prove the further lowering unambiguously because of the two experimental weaknesses in Ref. 21:

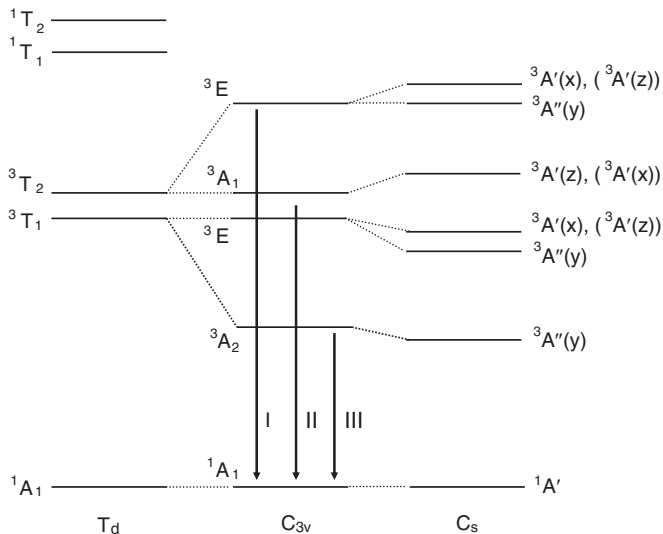


FIG. 1. A proposed energy-level diagram of the triplet STEs in PbMoO_4 . Because of the symmetry lowering from T_d to C_{3v} due to the JT effect, the 3T_2 state splits into the 3E and 3A_1 sublevels and the 3T_1 state into the 3E and 3A_2 sublevels. Owing to further symmetry lowering from C_{3v} to C_s , the 3E state transforms to the sublevels ${}^3A'(x)$ [or ${}^3A'(z)$] and ${}^3A''(y)$. The 3A_1 and 3A_2 states transform to the sublevels ${}^3A'(z)$ [or ${}^3A'(x)$] and ${}^3A''(y)$, respectively. The ${}^3A'(z)$ state derived from 3E and the ${}^3A'(x)$ state derived from 3A_1 are both a minor component (indicated in parentheses), if the crystal field is not so strong compared with the JT coupling. The radiative transitions giving rise to bands I, II, and III are indicated by arrows I, II, and III, respectively. Note that the energy separations are not on scale.

(i) bands II and III are closely situated to each other and
(ii) inevitably existing Mo-related defect luminescence largely masks the JT split intrinsic bands. Accordingly, it was rather difficult to decompose the time-resolved PbWO_4 luminescence spectra into three bands with sufficient reliability, which requires further extension of similar polarization experiments to other systems.

In the present study, we have investigated the polarization characteristics of time-resolved luminescence spectra of PbMoO_4 single crystals in which three bands peaking at 405 nm (I), 520 nm (II), and 600 nm (III) are well separated from each other.¹⁴ The PbMoO_4 crystal is also, in principle, free from Mo impurity defects. The three emission bands are significantly polarized in the ac plane, in support of the previous work on PbWO_4 . The results are explained by taking into account the compressive crystal field in combination with JT distortion. Based on the observed polarization characteristic of each band, the electronic structure of the triplet STE states in PbMoO_4 is group theoretically considered in some detail.

II. EXPERIMENT

The PbMoO_4 crystal is tetragonal, with the space group $I4_1/a$ ^{1,2} and therefore optically uniaxial. The optical axis is parallel to the crystallographic c axis, while the a and b axes are equivalent to each other.

Single crystals of PbMoO_4 used in the present experiment were obtained from Furukawa Co., Japan. They were grown

by the Czochralski technique from raw materials of PbO of 99.99% purity and MoO_3 of 99.9% purity in 1:1 molar ratio and purified by a three-time crystallization technique. The samples were polished to optical grade over all surfaces, having a size of $7 \times 6 \times 2 \text{ mm}^3$. The orientation of the crystal axes was determined by means of x-ray diffraction. A sample with the ac surface plane was mounted with its c axis horizontal on the copper holder that allowed for optical access in the horizontal plane. The sample holder was placed in a closed-cycle cryogenic refrigerator working in the temperature range between 8 and 300 K.

The fourth harmonics (266 nm) of a Q -switched neodymium-doped yttrium aluminum garnet (Nd:YAG) laser (Continuum Minilite II) was used as a pulsed light source, which corresponds to the high-energy region of the exciton absorption band in PbMoO_4 .²² The pulse width, repetition rate, and power density on the sample surface were 7 ns, 10 Hz, and 10 MW/cm^2 , respectively. An electronic synchronization technique using a digital delay-pulse generator (BNC Model 555) was applied to our time-resolved spectroscopy, without time jitter. The delay time τ_D was changed from 0 to 1 ms, with a gate width Δt ranging from 40 ns to 200 μs .

Since PbMoO_4 is a birefringent crystal, only light linearly polarized either parallel or perpendicular to the c axis preserves its polarization state on passing through the crystal, which restricts the determination of the polarization of luminescence to the components with the electric vector polarized parallel to the c axis ($\mathbf{E} \parallel \mathbf{c}$) and perpendicular to it ($\mathbf{E} \perp \mathbf{c}$). The polarization of laser light was varied in either direction of $\mathbf{E}_{\text{ex}} \parallel \mathbf{c}$ or $\mathbf{E}_{\text{ex}} \perp \mathbf{c}$ by using a half-wave plate. The incident angle of laser light was nearly normal to the sample surface, and luminescence signals from the irradiated surface were observed along the 30° direction relative to the laser beam. After passing through a linear polarizer, the luminescence was focused by a convex lens onto the entrance slit of a Jobin-Yvon HR320 monochromator equipped with a gated intensified charge-coupled device camera (Hamamatsu C5909-06), with a spectral resolution of 10 nm. A quartz depolarizer was used to eliminate any influence of the polarization characteristics of the analyzing system. The luminescence spectra obtained here were not corrected for the spectral response of the detection system.

III. RESULTS

Time-resolved luminescence spectra obtained under the excitation by photons polarized with $\mathbf{E}_{\text{ex}} \parallel \mathbf{c}$ and $\mathbf{E}_{\text{ex}} \perp \mathbf{c}$ at $T = 8 \text{ K}$ are shown in Figs. 2(a) and 2(b), respectively. Black and red curves correspond to the spectra for $\mathbf{E} \parallel \mathbf{c}$ and $\mathbf{E} \perp \mathbf{c}$, respectively. The intensities in Figs. 2(a) and 2(b) are normalized to unity at their maxima measured for $\mathbf{E} \parallel \mathbf{c}$. The spectra are broad and totally structureless. Remarkable changes in spectral shape and peak position are not seen in the range of $\tau_D = 50 \text{ ns} - 1 \text{ ms}$. One may see only the main band II, having a peak at 520 nm. No luminescence related to oxygen vacancy (MoO_3 group) is observed in our samples, although it is sometimes found in the red spectral region.⁸ Since band II is intense and has a long decay time ($\approx 4 \mu\text{s}$) at low temperatures ($T < 130 \text{ K}$),¹⁴ the other two bands, I and III, are completely masked by band II. Here, we shall define

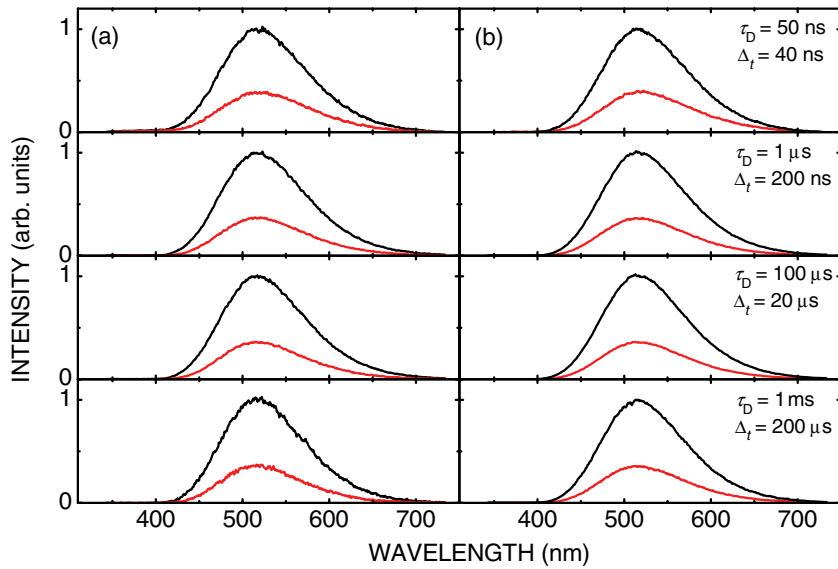


FIG. 2. (Color online) Time-resolved luminescence spectra measured for polarizations $\mathbf{E}\parallel\mathbf{c}$ (black line) and $\mathbf{E}\perp\mathbf{c}$ (red line) at $T = 8$ K. The excitation was made by 266-nm laser light polarized parallel to the c axis (a) and perpendicular to it (b). The spectra in (a) and (b) are normalized to unity at their maxima measured for $\mathbf{E}\parallel\mathbf{c}$, respectively.

the degree of polarization as

$$P = \frac{I(\mathbf{E}\parallel\mathbf{c}) - I(\mathbf{E}\perp\mathbf{c})}{I(\mathbf{E}\parallel\mathbf{c}) + I(\mathbf{E}\perp\mathbf{c})}, \quad (1)$$

where $I(\mathbf{E}\parallel\mathbf{c})$ and $I(\mathbf{E}\perp\mathbf{c})$ are the intensities of luminescence polarized along the directions $\mathbf{E}\parallel\mathbf{c}$ and $\mathbf{E}\perp\mathbf{c}$, respectively. From Figs. 2(a) and 2(b), it appears that the value of P does not change even if τ_D is varied within the range available in the present experiment. It is as large as $+0.48$, irrespective of polarizations $\mathbf{E}_{\text{ex}}\parallel\mathbf{c}$ and $\mathbf{E}_{\text{ex}}\perp\mathbf{c}$ of excitation light.

When T is increased to 150 K, the decay time of band II becomes comparable to or faster than those of bands I and III.¹⁴ It is thus possible to explicitly observe the composite nature of the PbMoO_4 luminescence in the temperature range of $T > 150$ K. Time-resolved luminescence spectra for $\mathbf{E}\parallel\mathbf{c}$ and $\mathbf{E}\perp\mathbf{c}$ observed under the excitation by photons polarized with $\mathbf{E}_{\text{ex}}\parallel\mathbf{c}$ at $T = 200$ K are shown in Figs. 3(a) and 3(b), respectively. Since the spectra measured at the same delay time are normalized to unity at their maxima, the relative intensities

of Figs. 3(a) and 3(b) are comparable to each other at their respective delay times.

A band peaking at 505 nm is seen just after the pulse excitation ($\tau_D = 50$ ns). This band corresponds to the main band II observed at 8 K. Its peak position is blueshifted by 15 nm when T is raised from 8 to 200 K. Such a blueshift of the triplet luminescence is a common feature in tungstates and molybdates.^{13,23,24} The spectra observed in the vicinity of $\tau_D = 1$ μs are decomposed into two individual bands II and III, which are indicated by green and orange lines, respectively. This decomposition is easily performed, because both bands are well separated from each other. Band I (indicated by violet line) is isolated at 405 nm and becomes observable in the range $\tau_D = 10$ μs – 100 μs . The sum of these bands is indicated by red lines, in satisfactorily good agreement with the experimental data. From comparison of Fig. 3(a) with Fig. 3(b), it is evident that the intensities of three bands in Fig. 3(b) are greater than those in Fig. 3(a), i.e., they are polarized with $\mathbf{E}\perp\mathbf{c}$. We obtain $P(\text{I}) = -(0.25 \pm 0.02)$, $P(\text{II}) = -(0.40 \pm 0.02)$, and P

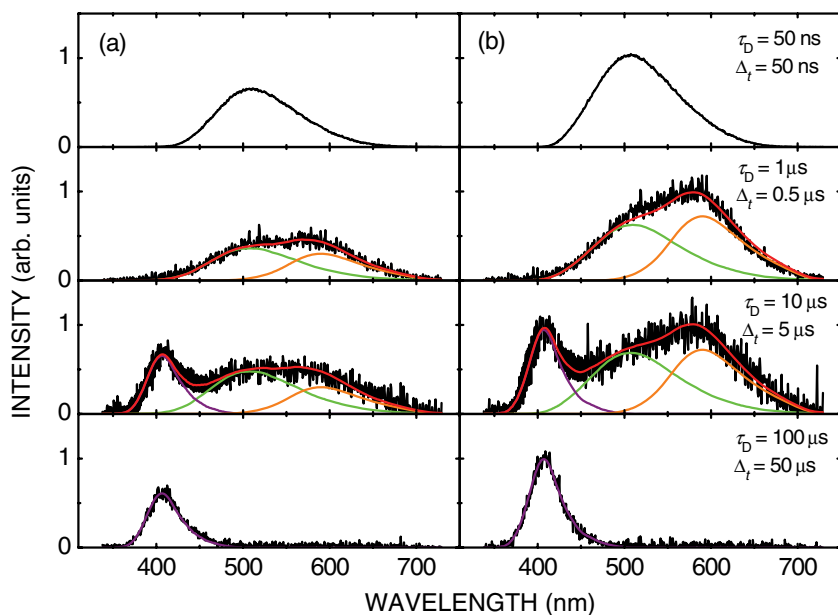


FIG. 3. (Color online) Time-resolved luminescence spectra for (a) $\mathbf{E}\parallel\mathbf{c}$ and (b) $\mathbf{E}\perp\mathbf{c}$ under the excitation by laser light polarized with $\mathbf{E}_{\text{ex}}\parallel\mathbf{c}$ at $T = 200$ K. Since the spectra measured at the same delay time are normalized to unity at their maxima, the relative intensities of (a) and (b) are comparable to each other at their respective delay times. Bands I, II, and III are depicted by violet, green, and orange lines, respectively. The sum of these three bands is indicated by red lines, in good agreement with the observed spectra.

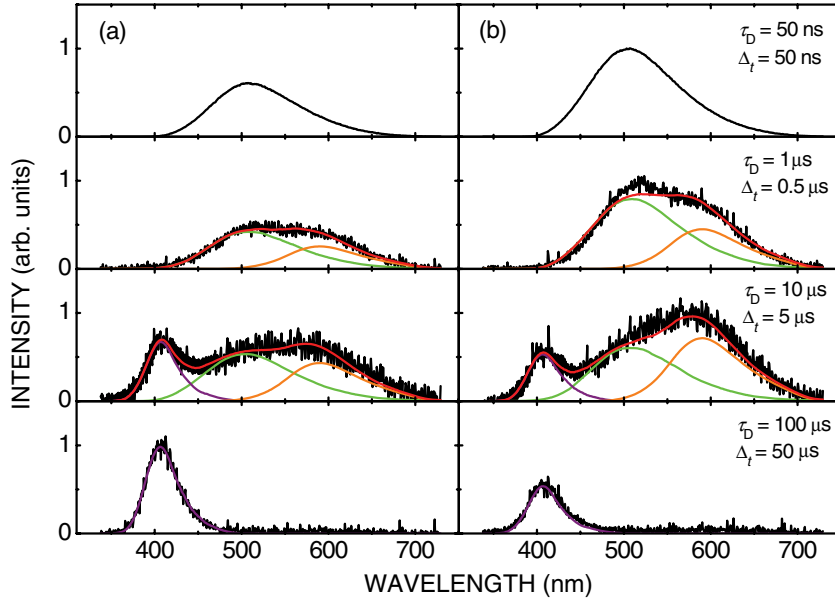


FIG. 4. (Color online) The same as in Fig. 3 but excited by laser light polarized with $\mathbf{E}_{\text{ex}} \perp \mathbf{c}$.

(III) = $-(0.32 \pm 0.04)$. The errors of P are evaluated from the uncertainty of the emission intensities due to the spectral decomposition into three bands.

Time-resolved luminescence spectra for $\mathbf{E} \parallel \mathbf{c}$ and $\mathbf{E} \perp \mathbf{c}$ observed under the excitation by photons polarized with $\mathbf{E}_{\text{ex}} \perp \mathbf{c}$ at $T = 200$ K are shown in Figs. 4(a) and 4(b), respectively. The color and line indications of the respective bands are the same as Fig. 3. Comparing Fig. 4(a) with Fig. 4(b), we obtain P (I) = $+(0.29 \pm 0.02)$, P (II) = $-(0.42 \pm 0.02)$, and P (III) = $-(0.32 \pm 0.04)$. The most striking feature to be noted in Figs. 2–4 is the polarization change of band II from $P > 0$ to $P < 0$ when T is increased from 8 to 200 K. The values of P do not depend on the polarization of excitation light, except for band I. This band is polarized in the $\mathbf{E} \perp \mathbf{c}$ direction under $\mathbf{E}_{\text{ex}} \parallel \mathbf{c}$ excitation and polarized in the $\mathbf{E} \parallel \mathbf{c}$ direction under $\mathbf{E}_{\text{ex}} \perp \mathbf{c}$ excitation.

Temperature dependence of P was investigated for all three bands under both polarizations of excitation light. The result of band II is presented in Fig. 5, where black open circles correspond to the data of $\mathbf{E}_{\text{ex}} \parallel \mathbf{c}$ and red closed circles to those of $\mathbf{E}_{\text{ex}} \perp \mathbf{c}$. Obviously, band II is primarily polarized with $\mathbf{E} \parallel \mathbf{c}$ at $T < 50$ K, having $P \approx +0.48$. With increasing temperature, the value of P begins to decrease at ~ 75 K, changes its sign from positive to negative at 125 K, and eventually reaches $-(0.50 \pm 0.03)$ at 225 K, irrespective of the polarization of excitation light. In Fig. 5, a solid line is the best-fitted curve of Eq. (4), described later.

As noted before, bands I and III are observable at $T > 150$ K. The temperature dependences of P of these bands are shown by circles and triangles in Fig. 6, respectively, where open symbols refer to the results of $\mathbf{E}_{\text{ex}} \parallel \mathbf{c}$ and closed symbols to those of $\mathbf{E}_{\text{ex}} \perp \mathbf{c}$. Solid lines are depicted as guides to the eye. The values of P of both bands are independent of the temperature in the range of $T = 150$ –225 K.

The polarization characteristics of bands I, II, and III observed here for PbMoO_4 are in good overall accord with those of the corresponding bands in PbWO_4 ,²¹ although the spectral decomposition into three bands was a difficult task in the latter case.

IV. DISCUSSION

The PbMoO_4 crystal possesses four crystallographically equivalent $(\text{MoO}_4)^{2-}$ tetrahedra per unit cell. Figure 7(a) shows a tetrahedral $(\text{MoO}_4)^{2-}$ ion with respect to the c axis, in which one molybdenum (Mo) ion and four oxygen (O_1 , O_2 , O_3 , and O_4) ions are depicted by open and gray circles, respectively. The projection of $(\text{MoO}_4)^{2-}$ tetrahedra onto the ab plane is also shown in Fig. 7(b). The direction of the oxygen bridge O_1 – O_2 (O_3 – O_4) in a $(\text{MoO}_4)^{2-}$ ion, lying in the ab plane, is rotated away by 30° from the a (b) axis.²⁵

As mentioned in the Introduction, the STE located on a $(\text{MoO}_4)^{2-}$ ion with T_d symmetry has two triplet states 3T_2 and 3T_1 , from which the intrinsic green luminescence is emitted. An isolated tetrahedral ion upon excitation is really subject

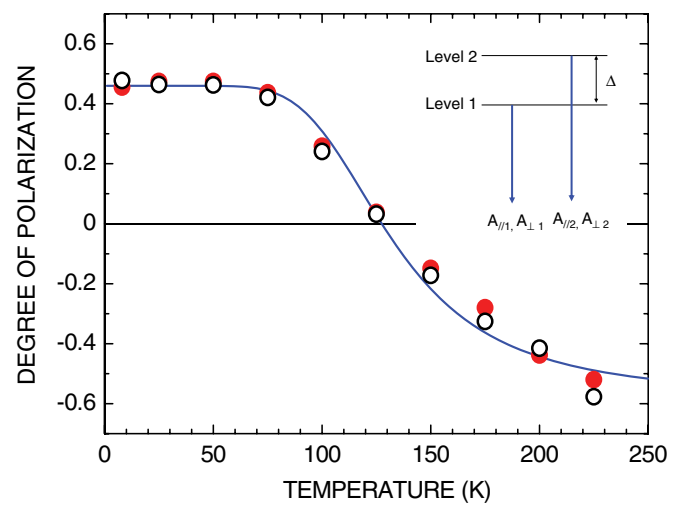


FIG. 5. (Color online) Temperature dependence of the degree of polarization of band II. Black open circles refer to the results measured under $\mathbf{E}_{\text{ex}} \parallel \mathbf{c}$ excitation and red closed circles to those under $\mathbf{E}_{\text{ex}} \perp \mathbf{c}$ excitation. The solid line is the best-fitted curve of Eq. (4) to the experimental points. The inset shows a two-level model to account for the thermal change of P , with the details described in the text.

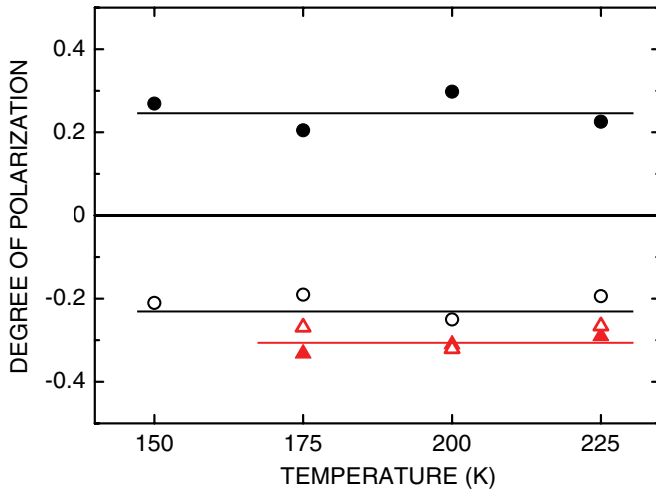


FIG. 6. (Color online) Temperature dependences of the degree of polarization of band I (black circles) and band III (red triangles). Open symbols refer to the results measured under $\mathbf{E}_{\text{ex}} \parallel \mathbf{c}$ excitation and closed symbols to those under $\mathbf{E}_{\text{ex}} \perp \mathbf{c}$ excitation. Solid lines are depicted as guides to the eye only.

to the JT instability, i.e., it tends to deform to a trigonal pyramid, in which one Mo–O bond is lengthened, while the other three Mo–O bonds are shortened. This trigonal pyramid has a threefold axis c_3 along the lengthened Mo–O bond. Since the trigonal JT distortion lowers the symmetry of $(\text{MoO}_4)^{2-}$ ions from T_d to C_{3v} , the degeneracy of the 3T_1 and 3T_2 states could be removed. The 3T_1 state splits into two sublevels with irreducible representations 3A_2 and 3E and the 3T_2 state into two sublevels with irreducible representations 3A_1 and 3E . The situation of this splitting is shown in the middle of Fig. 1, where the 3A_1 state and the 3E state stemming from 3T_1 are assumed to be close to each other in energy. Although a group-theoretical approach does not say anything about the order of each sublevel on an energy scale, bands I, II, and III are likely assigned to the radiative transitions from the sublevels

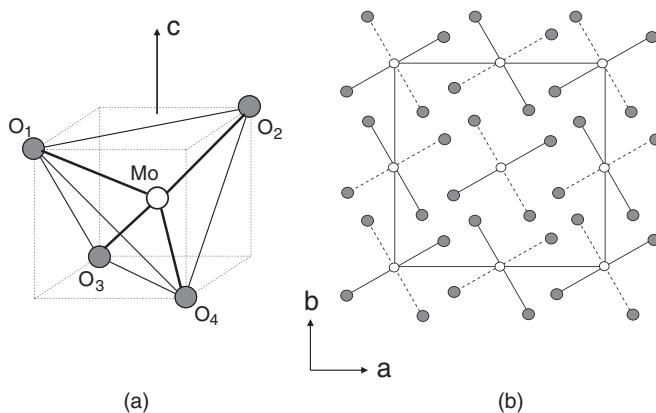


FIG. 7. (a) A tetrahedral $(\text{MoO}_4)^{2-}$ ion with respect to the crystallographic c axis. One molybdenum (Mo) ion and four oxygen (O_1 , O_2 , O_3 , and O_4) ions are depicted by open and gray circles, respectively. (b) Projection of the $(\text{MoO}_4)^{2-}$ tetrahedra onto the ab plane. Solid lines in $(\text{MoO}_4)^{2-}$ complexes are to oxygen atoms lying above the Mo atom and broken lines to oxygen atoms below the Mo atom.

3E , ${}^3A_1/{}^3E$, and 3A_2 , respectively.¹⁴ These transitions are indicated by arrows in Fig. 1.

The threefold axis c_3 of JT-distorted $(\text{MoO}_4)^{2-}$ ions does not coincide with the crystal c axis. Furthermore, it is worthwhile noticing that there are four equivalent threefold axes along Mo– O_1 , Mo– O_2 , Mo– O_3 , and Mo– O_4 bonds; that is, they can find each other by a rotation of 90, 180, and 270° about the c axis, respectively. This fact would result in the equality in intensity between the luminescence polarized parallel to the c axis and that perpendicular to it; $I(\mathbf{E} \parallel \mathbf{c}) = I(\mathbf{E} \perp \mathbf{c})$. Accordingly, although the appearance of three components is well accounted for by introducing the JT effect, no polarization with respect to the c axis is expected for the STE luminescence in PbMoO_4 as far as the $(\text{MoO}_4)^{2-}$ ion retains the C_{3v} symmetry. The observation of polarized luminescence, therefore, invokes a further lowering of the symmetry of $(\text{MoO}_4)^{2-}$ ions, which leads to $I(\mathbf{E} \parallel \mathbf{c}) \neq I(\mathbf{E} \perp \mathbf{c})$.

From a neutron diffraction experiment on scheelite molybdate crystals,²⁵ it is found that $(\text{MoO}_4)^{2-}$ tetrahedra are slightly distorted by a compression along the c axis. This tetragonal crystal field lowers the symmetry of $(\text{MoO}_4)^{2-}$ species in the ground state from T_d to D_{2d} . A combination of the JT coupling and the uniaxial crystal field could reduce the symmetry of $(\text{MoO}_4)^{2-}$ ions upon excitation from C_{3v} to C_s . In Fig. 8 are presented the orientations of the fine-structure axis (spin axis) for one of the excited $(\text{MoO}_4)^{2-}$ species with respect to the crystallographic axes and also relative to four oxygen ions in the ground state. The mirror plane σ_d spanned by O_1 –Mo– O_2 is the only symmetry element in C_s symmetry. The y fine-structure axis is almost perpendicular to the σ_d plane. The z fine-structure axis is close to being parallel to the Mo– O_1 bond and lies together with the x fine-structure axis approximately in the σ_d plane. The orientations x , y , and z of the transition dipole moments coincide, to a good approximation, with those of the corresponding fine-structure axes,¹⁸ both being not distinguished in this paper.

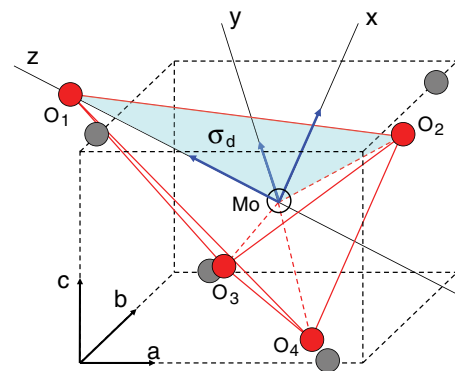


FIG. 8. (Color online) An excited $(\text{MoO}_4)^{2-}$ ion with C_s symmetry. One molybdenum (Mo) ion and four oxygen (O_1 , O_2 , O_3 , and O_4) ions are depicted by open and red circles in relation to the crystallographic axes, respectively. Four oxygen ions in the ground state are also shown by gray circles for reference. The mirror plane σ_d spanned by O_1 –Mo– O_2 is the only symmetry element in C_s symmetry. The y fine-structure axis is almost perpendicular to the σ_d plane. The z fine-structure axis is close to the direction of Mo– O_1 bond and lies together with the x fine-structure axis approximately in the σ_d plane.

The four excited states 3A_1 , 3E , 3A_2 , and 3E in C_{3v} symmetry transform under C_s symmetry as follows: ${}^3A_1 \rightarrow {}^3A'(\mathbf{x})$ or ${}^3A'(\mathbf{z})$, ${}^3E \rightarrow {}^3A''(\mathbf{y})$ and ${}^3A'(\mathbf{x})$ or ${}^3A'(\mathbf{z})$, and ${}^3A_2 \rightarrow {}^3A''(\mathbf{y})$, where the vectors \mathbf{x} , \mathbf{y} , and \mathbf{z} in parentheses correspond to the orientations x , y , and z of the transition dipole moments, respectively. The transitions from all the excited states of A' type and A'' type to the ground state of A' type are optically allowed. The influence of the spin-orbit interaction is thought to be negligibly small, because it is nearly restricted to the oxygen ligands.⁵

A complication arises because the dipole-moment axes x , y , and z do not coincide with the crystal axes a , b , and c . This problem can be resolved by taking into account the intensities of the \mathbf{x} -, \mathbf{y} -, and \mathbf{z} -polarized light are proportional to the square of the direction cosine θ of the respective angles with the crystal axes \mathbf{a} , \mathbf{b} , and \mathbf{c} . Fortunately, the values of $\cos \theta$ in PbMoO_4 can be evaluated from the structure parameters in Ref. 20. The \mathbf{x} -polarized light has $\cos \theta = 0.29$, 0.01 , and 0.96 with respect to \mathbf{a} , \mathbf{b} , and \mathbf{c} , respectively. The \mathbf{y} -polarized light has $\cos \theta = -0.53$ (\mathbf{a}), 0.84 (\mathbf{b}), and 0.10 (\mathbf{c}). The \mathbf{z} -polarized light has $\cos \theta = -0.82$ (\mathbf{a}), -0.51 (\mathbf{b}), and 0.28 (\mathbf{c}). From these results, it is reasonable to conclude that the \mathbf{x} -polarized light is a predominant component of $I(\mathbf{E}\parallel\mathbf{c})$, with a small contribution to $I(\mathbf{E}\perp\mathbf{c})$, whereas the \mathbf{y} - or \mathbf{z} -polarized light largely contributes to $I(\mathbf{E}\perp\mathbf{c})$, with a small amount of $I(\mathbf{E}\parallel\mathbf{c})$. Therefore, one can expect the observation of polarized luminescence with $P > 0$ for \mathbf{x} and with $P < 0$ for \mathbf{y} and \mathbf{z} .

The level transformation from C_{3v} to C_s is illustrated on the right side of Fig. 1. For scheelite CaMoO_4 ,¹⁸ it is pointed out that the compressive crystal field is considerably weak compared with the JT coupling, meaning that the symmetry lowering of $(\text{MoO}_4)^{2-}$ ions from C_{3v} to C_s is not so significant. We are convinced that this also holds for PbMoO_4 . If the crystal field were not the dominant factor in lifting the degeneracy, among ${}^3A'(\mathbf{x})$ and ${}^3A'(\mathbf{z})$ derived from 3A_1 , the latter would be more predominant than the former, and among ${}^3A'(\mathbf{x})$ and ${}^3A'(\mathbf{z})$ derived from 3E , the former would become a major component. In Fig. 1, minor components are enclosed in parentheses. Consequently, it seems likely from Fig. 1 that state I consists of two sublevels ${}^3A'(\mathbf{x})$ [$P > 0$] and ${}^3A''(\mathbf{y})$ [$P < 0$], state II of three sublevels ${}^3A'(\mathbf{z})$ [$P < 0$], ${}^3A'(\mathbf{x})$ [$P > 0$], and ${}^3A''(\mathbf{y})$ [$P < 0$], and state III of a single sublevel ${}^3A''(\mathbf{y})$ [$P < 0$]. These three states, I, II, and III, might correspond to three minima of the multidimensional adiabatic potential energy surface calculated for the excited triplet states in tetrahedral complexes.^{16,17}

By referring to the above group-theoretical considerations, we first discuss the electronic structure of the luminescent triplet state responsible for main band II. This band is primarily polarized with the electric vector along the c axis at low temperatures but changes its polarization from $\mathbf{E}\parallel\mathbf{c}$ to $\mathbf{E}\perp\mathbf{c}$ at $T > 125$ K, as shown in Fig. 5. A similar temperature-dependent degree of polarization has been reported for PbMoO_4 by Reut,²⁶ who investigated the polarization of total (i.e., time-integrated) luminescence under steady-state excitation in the range $T = 70$ – 320 K. The time-integrated luminescence is surely dominated by band II.

The result of Fig. 5 clearly suggests that at least two excited states having an opposite polarization contribute to the main band. It can be explained in terms of a two-level

model presented by the inset. The upper level is labeled 2, and the lower (metastable) level is labeled 1, both of which are separated by an energy Δ . Optically excited electrons are assumed to be preferentially populated on lower level 1 at low temperatures. An increase in temperature will result in the thermal population of upper level 2. In such a two-level model, the intensities of luminescence components polarized in the $\mathbf{E}\parallel\mathbf{c}$ and $\mathbf{E}\perp\mathbf{c}$ directions may be simply given as

$$I(\mathbf{E}\parallel\mathbf{c}) = A_{\parallel 1} + A_{\parallel 2} \exp(-\Delta/k_B T), \quad (2)$$

and

$$I(\mathbf{E}\perp\mathbf{c}) = A_{\perp 1} + A_{\perp 2} \exp(-\Delta/k_B T), \quad (3)$$

respectively, where $A_{\parallel 1}$ and $A_{\perp 1}$ are the radiative transition probabilities from level 1 in the direction parallel and perpendicular to the c axis, respectively, $A_{\parallel 2}$ and $A_{\perp 2}$ are the corresponding ones from level 2, and k_B is the Boltzmann constant. By substituting Eqs. (2) and (3) into Eq. (1), one obtains

$$P = \frac{(A_{\parallel 1} - A_{\perp 1}) + (A_{\parallel 2} - A_{\perp 2}) \exp(-\Delta/k_B T)}{(A_{\parallel 1} + A_{\perp 1}) + (A_{\parallel 2} + A_{\perp 2}) \exp(-\Delta/k_B T)}. \quad (4)$$

The total transition probability ($A_{\parallel 1} + A_{\perp 1}$) from level 1 is not clear from the present experiment, and therefore it is normalized to unity. The solid line in Fig. 5 is the best-fitted curve of Eq. (4) to the experimental points. The goodness of fit is obvious. From this fit, we obtain $(A_{\parallel 1} - A_{\perp 1}) = 0.46 \pm 0.04$, $(A_{\parallel 2} + A_{\perp 2}) = 200 \pm 20$, $(A_{\parallel 2} - A_{\perp 2}) = -(120 \pm 20)$, and $\Delta = 61 \pm 5$ meV. The present value of Δ is a bit smaller than the result (74 meV) by Reut.²⁶ Level 1 has a polarization characteristic $P > 0$ since $A_{\parallel 1} > A_{\perp 1}$, whereas level 2 is characterized by $P < 0$ since $A_{\perp 2} > A_{\parallel 2}$. That is to say, two excited states giving rise to main band II have an opposite polarization, as expected. The total transition probability from level 2 is much greater than that from level 1; $(A_{\parallel 2} + A_{\perp 2}) \gg 1$. This is to be expected from the appreciable change of polarization from positive to negative by raising the temperature.

At high temperatures, a question arises because of the onset of thermal quenching of the STE luminescence. This quenching is attributed to thermal disintegration of STEs or nonradiative transitions from the luminescent state to the ground state. There may be a competition between the quenching phenomenon and the thermal change in population between two sublevels. In PbMoO_4 , the intensity of the green luminescence begins to decrease at around 130 K, with the activation energy $\Delta E \approx 260$ meV.²⁷ On the other hand, the polarization change of band II starts at $T \approx 75$ K with $\Delta = 61$ meV. The value of Δ is more than four times smaller than ΔE . Therefore, it is likely supposed that the temperature dependence of P of band II is hardly influenced by the thermal quenching phenomenon. A similar situation is also found in PbWO_4 ²¹ and CdMoO_4 .¹⁵

There is an interesting finding on the main band II. Babin *et al.*²⁷ have revealed that the green luminescence in PbMoO_4 shows an order of magnitude increase of the decay time at very low temperatures ($T < 1$ K). This fact indicates the presence of a pair of closely spaced energy levels. The energy distance δ separating both levels is estimated to be 0.37 meV. If this observation is taken into consideration, it may be supposed

that the metastable level I is composed of two sublevels spaced closely in energy. The lowest-lying sublevel presumably has a small radiative transition probability, because its decay time is very long.²⁷

The above analysis leads us to a suggestion that luminescent state II consists of three sublevels separated by Δ and δ , where $\Delta \gg \delta$. This seems fairly consistent with the energy-level diagram in Fig. 1, where the closely spaced ${}^3A_1/{}^3E$ state responsible for band II splits into three sublevels ${}^3A'(z)$, ${}^3A'(x)$, and ${}^3A''(y)$ under C_s symmetry. The negatively polarized levels ${}^3A'(z)$ and ${}^3A''(y)$ locate 61 meV above and 0.37 meV below the positively polarized level ${}^3A'(x)$, respectively. At moderately low temperatures ($T \approx 8\text{--}75$ K), thermal equilibrium between ${}^3A'(x)$ and ${}^3A''(y)$ is achieved, and the resulting luminescence could be polarized with $\mathbf{E} \parallel \mathbf{c}$, because the radiative transition probability of level ${}^3A''(y)$ is considerably smaller than that of level ${}^3A'(x)$. For very low temperatures ($T < 1$ K), however, the existence of level ${}^3A''(y)$ is no longer negligible, i.e., the amount of P is expected to reduce to some extent. This is an intriguing subject to be examined in the future. When T is increased above 125 K, the population of level ${}^3A'(z)$ with large transition probability becomes significant, which results in the polarization change from $\mathbf{E} \parallel \mathbf{c}$ to $\mathbf{E} \perp \mathbf{c}$.

Band III gives a negative value of P as large as -0.3 . This value is independent of the polarization of excitation light and also the temperature, indicating the simple nature of band III. These polarization characteristics are in good agreement with our group-theoretical proposal in Fig. 1. The excited state giving rise to band III is attributed to the 3A_2 state in C_{3v} symmetry, and this state further transforms to a single sublevel ${}^3A''(y)$ under C_s symmetry, from which the negatively polarized luminescence is produced.

The polarization characteristic of band I is somewhat peculiar. It exhibits $P < 0$ or $P > 0$, depending on whether the excitation light is polarized with $\mathbf{E}_{\text{ex}} \parallel \mathbf{c}$ or $\mathbf{E}_{\text{ex}} \perp \mathbf{c}$. This fact imposes two requirements: (1) luminescent state I consists of two excited states having an opposite polarization, and (2) the polarization memory of excitation light is preserved in the course of the nonradiative relaxation from optically created states to the emitting states.

Requirement (1) may be fulfilled. As indicated in Fig. 1, the excited state responsible for band I is assigned to the 3E state in C_{3v} symmetry. Under C_s symmetry, this state further splits into two sublevels ${}^3A'(x)$ and ${}^3A''(y)$ separated by only a small energy difference; the former is polarized with $\mathbf{E} \parallel \mathbf{c}$ and the latter with $\mathbf{E} \perp \mathbf{c}$. Realization of (2), however, is not so frequent in ionic materials like transition-metal molybdates, i.e., optically created electrons lose their polarization memory due to the strong coupling with lattice vibrations.²⁸ Even if such depolarization efficiently takes place during the nonradiative relaxation process, one can observe polarized luminescence as far as the emitting state holds the proper polarization nature, which is really the case for bands II and III. On the other hand, band I differs from the other two bands in two aspects. First, its peak energy is the highest among the three bands, suggesting that the relaxation energy of optically created electrons into the luminescent state I is relatively small. Second, its band width is remarkably narrow compared with those of bands II and III, which implies a weak coupling

of electrons in state I with lattice vibrations. The situation concerning band I is more complicated. Although the same puzzle has also been found in PbWO_4 ,²¹ more studies are needed to answer the question why requirement (2) is met for band I.

Finally, we shall give a brief comment on the role of lead ions. Reflection spectra of PbMoO_4 and PbWO_4 crystals exhibit a pronounced exciton structure with distinct dichroism in the vicinity of the fundamental absorption edge.^{22,29} This structure is most likely explained as being due to the intracationic $\text{Pb } 6s \rightarrow 6p$ transition, indicating that the $\text{Pb } 6s$ and $6p$ states appreciably contribute to the top of the valence band composed of the $\text{O } 2p$ state and the bottom of the conduction band composed of the $\text{Mo } 4d$ ($\text{W } 5d$) state, respectively. We suppose that optically created excitons in PbMoO_4 (PbWO_4) move freely through the crystal within their lifetimes and then self-trap at $(\text{MoO}_4)^{2-}$ [$(\text{WO}_4)^{2-}$] ions by inducing the trigonal JT lattice deformation around themselves. It is not certain whether the lead character is lost during the migration and/or self-trapping processes of a free exciton. To keep things simple, the present discussions are made by assuming implicitly that the electronic states of STEs in PbMoO_4 have no contribution from lead ions. In PbWO_4 , the intrinsic self-trapped electron center, $(\text{WO}_4)^{3-}$, has been found by electron spin-resonance experiments.^{30,31} This center is formed as a result of the self-trapping of an electron at the regular lattice site of a W^{6+} ion. The electron self-trapping was first confirmed to occur in PbCl_2 ,³² in which an electron is trapped at a pair of nearest-neighbor Pb^{2+} ions, forming the $(\text{Pb}_2)^{3+}$ center. The trapping of holes at the regular oxygen ions in the vicinity of various perturbing defects has quite recently been revealed in $\text{PbWO}_4:\text{Mo},\text{La}(\text{Y})$ single crystals.³³ It is very interesting to investigate whether our assumption is really valid in lead compounds PbMoO_4 and PbWO_4 .

V. SUMMARY

In the present work, we have studied the electronic structure of the STE located on a tetrahedral oxyanion molecule by investigating the polarization characteristics of time-resolved luminescence spectra of oriented PbMoO_4 crystals over an 8–225 K temperature range. The obtained results provide us with more reliable information than the previous work on PbWO_4 .²¹ Three time-resolved bands, I, II, and III, are confirmed to be characteristically polarized with respect to the crystal c axis. It is stressed that the symmetry lowering of tetrahedral $(\text{MoO}_4)^{2-}$ ions due to the JT effect is rather insufficient to account for the polarization properties of these bands. Further lowering of the symmetry of $(\text{MoO}_4)^{2-}$ ions due to the uniaxial crystal field should be included. The sublevels of the luminescent triplet STE states responsible for bands I, II, and III are assigned on the basis of group-theoretical considerations, with a realistic assumption that the crystal field is considerably weak compared with the JT coupling. Band I originates from the excited state consisting of two sublevels ${}^3A'(x)$ and ${}^3A''(y)$, band II of three sublevels ${}^3A'(z)$, ${}^3A'(x)$, and ${}^3A''(y)$, and band III of a single sublevel ${}^3A''(y)$. Although the electronic structure of the triplet STE in PbMoO_4 is clarified to a certain extent by the present experiment, some unsettled subjects are proposed for future studies.

ACKNOWLEDGMENTS

The authors wish to express their sincere thanks to M. Fujita for invaluable advice and fruitful discussions

throughout the present research program on polarized luminescence in tungstates and molybdates. They are also indebted to S. Matsubayashi, K. Kasashima, Y. Kashiwai, and R. Matsumoto for assistance in the experiments.

*Corresponding author: itohlab@shinshu-u.ac.jp

¹R. W. G. Wyckoff, *Crystal Structures*, 2nd ed. (Wiley, New York, 1965), Vol. 3, Chap. 8.

²P. F. Schofield, K. S. Knight, S. A. T. Redfern, and G. Cressey, *Acta Crystallogr. Sec. B* **53**, 102 (1997).

³M. Nikl, V. V. Laguta, and A. Vedda, *Phys. Status Solidi B* **245**, 1701 (2008).

⁴G. Blasse, in *Structure and Bonding* (Springer, Berlin, 1980), Vol. 42, p. 1.

⁵C. J. Ballhausen, *Theor. Chim. Acta* **1**, 285 (1963).

⁶W. van Loo, *Phys. Status Solidi A* **28**, 227 (1975).

⁷E. G. Reut, *Izv. Akad. Nauk SSSR, Ser. Fiz. [Bull. Acad. Sci. USSR, Phys. Ser.]* **43**, 1186 (1979).

⁸J. A. Groenink and G. Blasse, *J. Solid State Chem.* **32**, 9 (1980).

⁹M. Nikl, P. Bohacek, E. Mihokova, M. Kobayashi, M. Ishii, Y. Usuki, V. Babin, A. Stolovich, S. Zazubovich, and M. Bacci, *J. Lumin.* **87–89**, 1136 (2000).

¹⁰A. Kotlov, L. Jönsson, H. Kraus, V. Mikhailik, V. Nagirnyi, G. Svensson, and B. I. Zadneprovski, *Radiat. Meas.* **42**, 767 (2007).

¹¹M. D. Sturge, in *Solid State Physics*, edited by F. Seitz, D. Turnbull, and H. Ehrenreich (Academic, New York, 1967), Vol. 20, p. 21.

¹²M. Itoh and T. Sakurai, *Phys. Status Solidi B* **242**, R52 (2005).

¹³M. Itoh and T. Sakurai, *Phys. Rev. B* **73**, 235106 (2006).

¹⁴T. Kajitani and M. Itoh, *Phys. Status Solidi C* **8**, 108 (2011).

¹⁵M. Itoh, *J. Lumin.* **132**, 645 (2012).

¹⁶M. Bacci, S. Porcinai, E. Mihóková, M. Nikl, and K. Polák, *Phys. Rev. B* **64**, 104302 (2001).

¹⁷M. Bacci, E. Mihóková, and L. S. Schulman, *Phys. Rev. B* **66**, 132301 (2002).

¹⁸W. Barendswaard and J. H. van der Waals, *Mol. Phys.* **59**, 337 (1986).

¹⁹J. van Tol, J. A. van Hulst, and J. H. van der Waals, *Mol. Phys.* **76**, 547 (1992).

²⁰J. van Tol and J. H. van der Waals, *Mol. Phys.* **88**, 803 (1996).

²¹M. Itoh and T. Aoki, *J. Phys.: Condens. Matter* **22**, 045503 (2010).

²²M. Fujita, M. Itoh, H. Mitani, Sangeeta, and M. Tyagi, *Phys. Status Solidi B* **247**, 405 (2010).

²³D. A. Spassky, S. N. Ivanov, V. N. Kolobanov, V. V. Mikhailin, V. N. Zemskov, B. I. Zadneprovski, and L. I. Potkin, *Radiat. Meas.* **38**, 607 (2004).

²⁴V. B. Mikhailik, H. Kraus, D. Wahl, M. Itoh, M. Koike, and I. K. Bailiff, *Phys. Rev. B* **69**, 205110 (2004).

²⁵E. Gürmen, E. Daniels, and J. S. King, *J. Chem. Phys.* **55**, 1093 (1971).

²⁶E. G. Reut, *Opt. Spektrosk.* **57**, 147 (1984) [*Opt. Spectrosc. (USSR)* **57**, 90 (1984)].

²⁷V. Babin, P. Bohacek, E. Bender, A. Krasnikov, E. Mihokova, M. Nikl, N. Senguttuvan, A. Stolovits, Y. Usuki, and S. Zazubovich, *Radiat. Meas.* **38**, 533 (2004).

²⁸Y. Toyozawa, *Optical Processes in Solids* (Cambridge University Press, Cambridge, 2003), Chap. 4.

²⁹M. Fujita, M. Itoh, M. Horimoto, and H. Yokota, *Phys. Rev. B* **65**, 195105 (2002).

³⁰V. V. Laguta, J. Rosa, M. I. Zariskii, M. Nikl, and Y. Usuki, *J. Phys.: Condens. Matter* **10**, 7293 (1998).

³¹M. Böhm, F. Henecker, A. Hofsaettter, M. Luh, B. K. Meyer, A. Scharmann, O. V. Kondratiev, and M. V. Korzhik, *Radiat. Eff. Defects Solids* **150**, 21 (1999).

³²S. V. Nistor, E. Goovaerts, and D. Schoemaker, *Phys. Rev. B* **48**, 9575 (1993).

³³V. V. Laguta, M. Buryi, M. Nikl, J. Rosa, and S. Zazubovich, *Phys. Rev. B* **83**, 094123 (2011).